# A UNIFIED METHOD FOR CHARACTERIZATION OF MICROSTRIP AND WAVEGUIDE DISCONTINUITIES OF IRREGULAR SHAPE †

Tzyy-Sheng Horng

Electrical Engineering Department, National Sun Yat-Sen University, Kaohsiung, Taiwan 80424, R.O.C.

† This research was supported by the National Science Council, R.O.C., under grant NSC85-2221-E-110-004.

## Abstract

A unified numerical method is proposed to analyze the discontinuities of two major waveguide structures, microstrips and rectangular waveguides, at microwave frequencies. Roof-top and rectangular-pipe subdomain functions are used in an electric-field integral-equation formulation to adequately expand the three-dimensional current densities of an irregularly-shaped conductor. It is therefore applicable to general configurations of microstrip and waveguide discontinuities. Shielded microstrips, which are combination of microstrips and rectangular waveguides, can be evaluated efficiently using this technique.

## I. Introduction

It was well known in the past that modal analysis techniques were used extensively to analyze all kinds of waveguide discontinuities [1]-[5]. For characterization of microstrip discontinuities, the most general solution was governed by the integral-equation modeling techniques such as the electric-field integral equation (EFIE) [6]-[8] and mixed-potential integral equation [9],[10]. These techniques require derivation of multilayered Green's functions and adopt proper current expansion functions in the numerical procedure. The earlier approaches to microstrip discontinuities were limited to a planar configuration due to an insufficient segmentation scheme for vertically directed component of current density. This was conquered recently with development of new types of expansion functions and has many applications on evaluation of via-holes and air-bridges [11]-[14]. In the previous work [15], a generalized method was given to find the three-dimensional current density inside a microstrip discontinuity considering finite thickness. The present work extends this technique to analyze rectangular waveguides of irregular shape as shown in Fig. 1. All the conducting walls can be considered very practically to have finite thickness and conductivity. In addition, as shown in Fig. 2, a novel structure combining rectangular waveguides, microstrips, and slots can be also investigated effectively using the same technique.

## II. Theory

As illustrated in Fig. 3, for a rectangular waveguide with finite conductor thickness, the corresponding three dimensional current distribution can be discretized into horizontally directed surface current densities on several layers plus vertically directed volume current densities between any two layers [15]. In this analysis roof-top subdomain functions are used to expand the horizontally directed surface current densities while rectangular-pipe subdomain functions are used to expand the volume current densities. They are mathematically expressed as

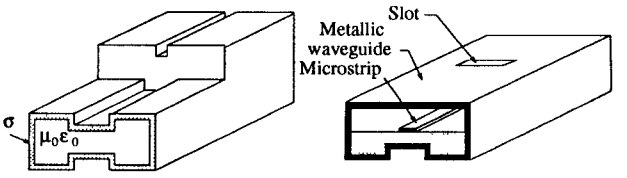


Fig. 1 (Left) Rectangular waveguide discontinuities of irregular shape. Fig. 2 (Right) A structure combining rectangular waveguide, microstrip, and slot.

$$\vec{J} = \hat{x}J_x + \hat{y}J_y + \hat{z}J_z \tag{1}$$

$$J_x(x,y,z) = \sum_{m,n,l} \frac{I_x^{m,n,l}}{d_y} T(\frac{x-md_x}{d_x}) P(\frac{y-(n-0.5)d_y}{d_y}) \cdot \delta(z-ld_z), \tag{2}$$

$$J_y(x,y,z) = \sum_{m,n,l} \frac{I_y^{m,n,l}}{d_x} P(\frac{x-(m-0.5)d_x}{d_x}) T(\frac{y-nd_y}{d_y}) \cdot \delta(z-ld_z), \tag{3}$$

$$J_z(x,y,z) = \sum_{m,n,l} \frac{I_z}{d_x d_y} P(\frac{x-(m-0.5)d_x}{d_x}) P(\frac{y-(n-0.5)d_y}{d_y}) \cdot P(\frac{z-(l-0.5)d_z}{d_z}) \tag{4}$$

where

$$T(u) = \begin{cases} 1-|u|, & |u| \le 1 \\ 0, & |u| > 1, \end{cases} \tag{5}$$

and

$$P(u) = \begin{cases} 1, & |u| \le \frac{1}{2} \\ 0, & |u| > \frac{1}{2}. \end{cases} \quad (6)$$

Note that $(md_x, nd_y, ld_z)$ represents the position of each grid point. To formulate an electric-field integral equation, the spectral-domain dyadic Green's function due to both horizontally and vertically directed Hertzian dipoles in a multilayered medium has been used. This integral equation is generally expressed as

$$\vec{E}_{exc}(x,y,z) + \frac{1}{4\pi^2}\int_{-\infty}^{\infty}\int_{-\infty}^{\infty}\int_{z'}\overline{\overline{G}}(k_x,k_y,z,z')\cdot\vec{J}(k_x,k_y,z') \cdot e^{-jk_x x}e^{-jk_y y}dz'\,dk_x dk_y = \frac{\vec{J}(x,y,z)}{\sigma} \quad (7)$$

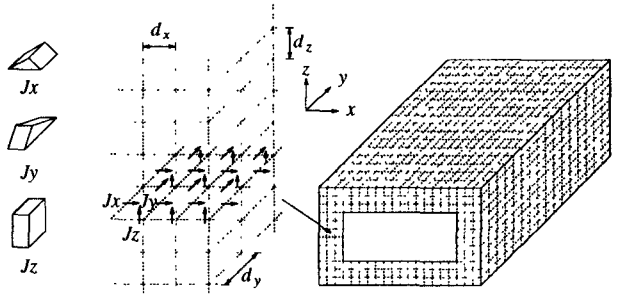


Fig. 3 Illustration of current discretization procedure for a rectangular waveguide.

where $\overline{\overline{G}}$ and $\vec{J}$ denote spectral-domain dyadic Green's function and Fourier transforms of the current densities respectively. $\vec{E}_{exc}$ is the impressed field for excitation and $\sigma$ is the conductivity of the conductor. The equation above implies that the rectangular waveguide can be embedded in a substrate. In addition, the same technique can be extended to complicated microstrip problems such as a microstrip discontinuity housed with a rectangular waveguide. The Galerkin procedure is finally applied to transform (7) into a matrix in the form

$$\begin{bmatrix} [Z_{J_xJ_x}] & [Z_{J_yJ_x}] & [Z_{J_zJ_x}] \\ [Z_{J_xJ_y}] & [Z_{J_yJ_y}] & [Z_{J_zJ_y}] \\ [Z_{J_xJ_z}] & [Z_{J_yJ_z}] & [Z_{J_zJ_z}] \end{bmatrix} \begin{bmatrix} [I_x] \\ [I_y] \\ [I_z] \end{bmatrix} = \begin{bmatrix} [V_x] \\ [V_y] \\ [V_z] \end{bmatrix}. \quad (8)$$

More detailed expressions associated with the impedance submatrices in (8) can be referred to [14]. For exciting the rectangular waveguide, a delta-gap voltage source is usually impressed across an additional vertically directed element between two horizontal walls. Similarly, for exciting the microstrip, the voltage source is placed between the signal line and ground plane. Through a simple matrix inversion, the current distribution and subsequently the scattering parameters of a discontinuity can be found.

## III. Numerical Results and Discussion

Fig 4 shows a rectangular waveguide which is open-ended for radiating into the space. The waveguide is excited using a voltage source placed between two horizontal walls. Figs. 5 and 6 illustrate the current density distributions on the top horizontal wall when the waveguide is excited below and above the cut-off frequency of the dominant mode ($TE_{10}$) respectively. The equivalent conductance and susceptance of the discontinuity can be further extracted from the current density distribution and their quantities are shown in Fig. 7. It can be seen that the calculated data agree very well with the curves published in the well-known reference The Waveguide Handbook [1].

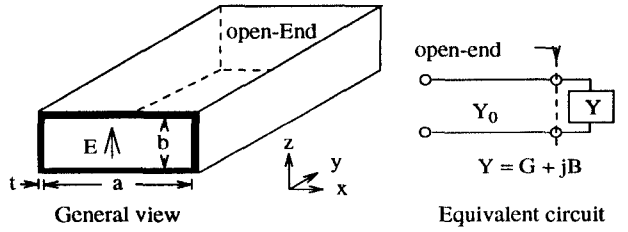


Fig. 4 The open-ended rectangular waveguide and its equivalent circuit. (a=900mil, t=100 mil, $\sigma = 5.8 \times 10^7$ S/m)

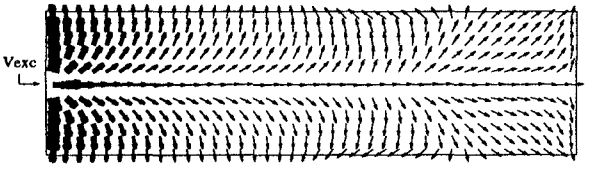


Fig. 5 The current density distribution on the top horizontal wall at the frequency of 5 GHz.

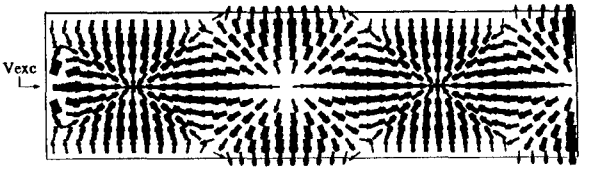


Fig. 6 The current density distribution on the top horizontal wall at the frequency of 8 GHz.

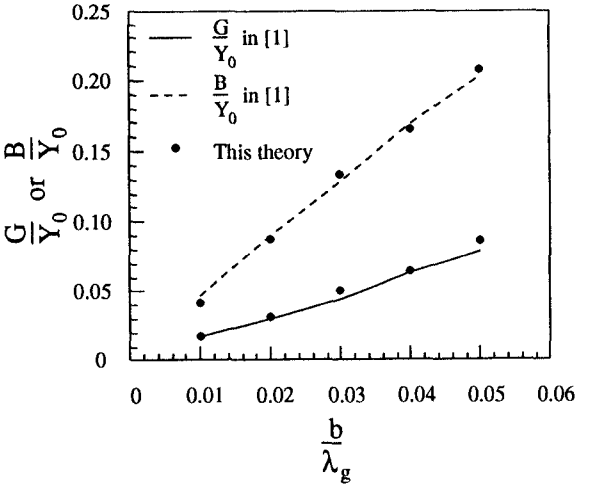


Fig. 7 Normalized conductance and susceptance for the open-ended rectangular waveguide.

Multi-terminal waveguide structures are also investigated. Fig. 8 shows a right-angle junction of two rectangular waveguides with equal dimensions. As suggested in [1], the equivalent circuit at the reference planes $T$ can be looked upon as a pure shunt capacitance. The corresponding susceptance and the location of the reference planes are calculated and shown in Fig. 9. When compared with those given in [1], good agreement is observed. An example of the current density plot on the top horizontal wall of this configuration is shown in Fig. 10.

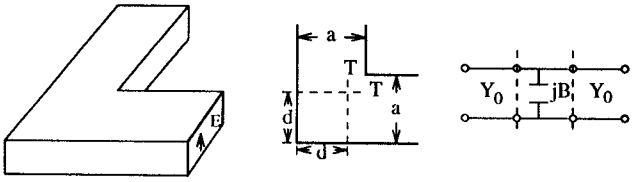


Fig. 8 A right-angle junction of two rectangular waveguides. (a=900mil, t=100 mil, $\sigma = 5.8 \times 10^7$ S/m)

Fig. 11 shows a T-type junction of three rectangular waveguides of equal dimensions. Similarly, an equivalent shunt reactance can be obtained as the terminals are assumed to have characteristic impedance $Z_0$ and $Z_0'$ with the reference plane $T$ and $T'$ respectively. In Fig. 12 quantities of the equivalent circuit parameters for the T junction are presented. Again, comparison of the results with those given in [1] shows excellent agreement.

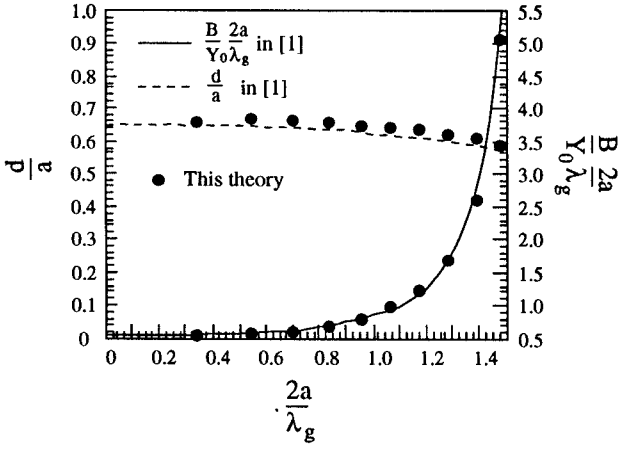


Fig. 9 Normalized susceptance and offsets of the reference planes for the right-angle junction of two rectangular waveguides.

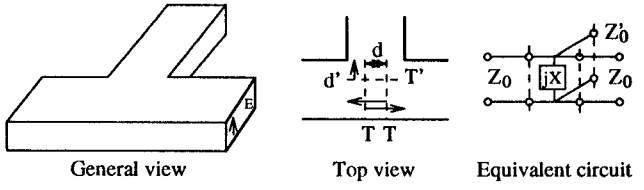


Fig. 11 A T-junction of three rectangular waveguides. (a=900mil, t=100 mil, $\sigma = 5.8 \times 10^7$ S/m)

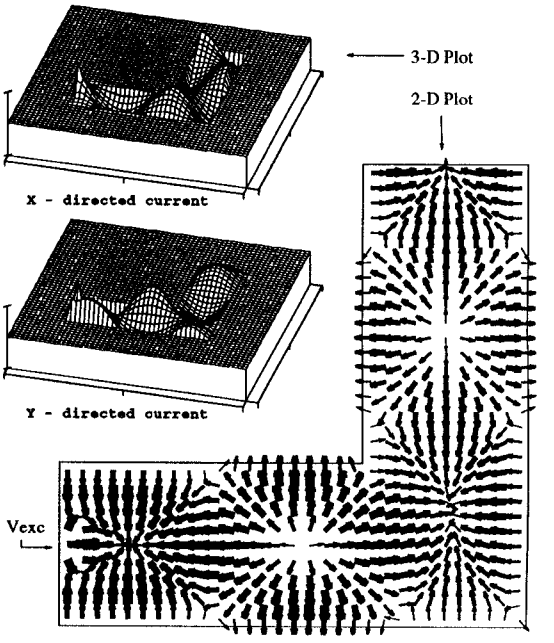


Fig. 10 The current density distribution on the top horizontal wall at the frequency of 8 GHz for the right-angle junction of two rectangular waveguides.

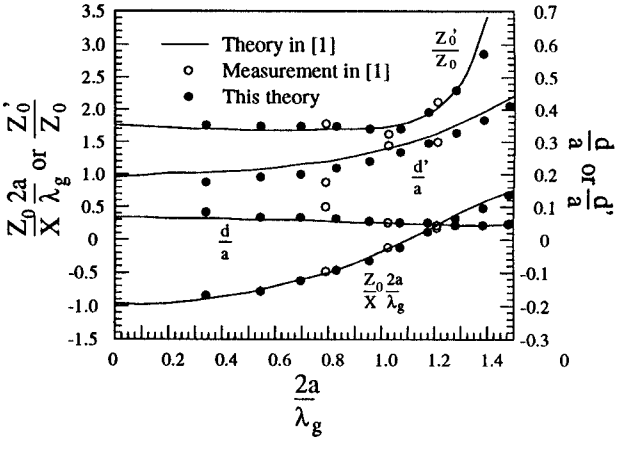


Fig. 12 Normalized impedances and offsets of the reference planes for the T junction of three rectangular waveguides.

The same theory is extended to microstrip discontinuity problems. As shown in Fig. 13, the microstrip open-end effects in open, covered, and shielded structures were studied. It can be seen that among three cases the curve of $< S_{11}$ for the open-end in a shielded structure has the least deviation from zero degree, which represents to have the smallest fringing field capacitance. The phase curves for the open and covered cases are further verified by the results generated using HPEEsof's Momentum software. Fig. 14 demonstrates

the current distributions on the microstrip as well as on the top horizontal wall of the waveguide at the frequency of 20 GHz. To prove the accuracy of analysis of shielded microstrip discontinuities using this theory, a double step discontinuity is investigated and the results shown in Fig. 15 are compared with the calculated and experimental data given in [16]. The agreement is still reasonably good.

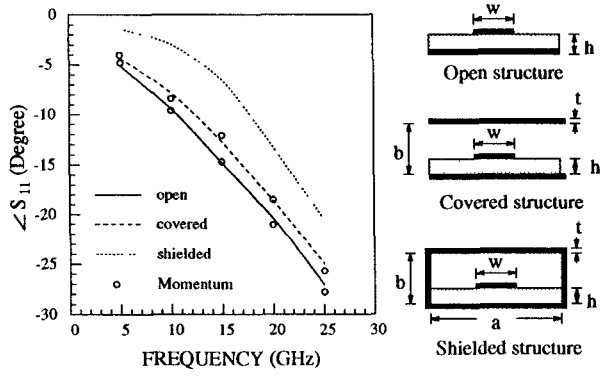


Fig. 13 The simulated phase of $S_{11}$ of a microstrip open-end in open, covered, and shielded structures. (a=3.5 mm, h=0.5 mm b=2 mm, w=1 mm, t=0.25 mm, $\sigma = 5.8 \times 10^7$, $\epsilon_r$=9.0)

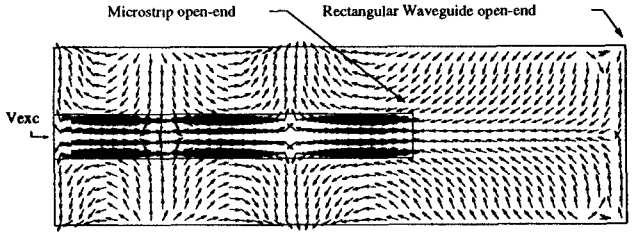


Fig. 14 Current density distributions on the microstrip and the top horizontal wall of the rectangular waveguide for a shielded open-end structure.

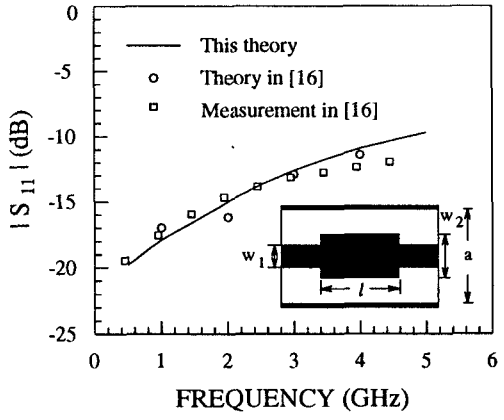


Fig. 15 Magnitude of $S_{11}$ of a microstrip double step discontinuity in a shielded structure. (a=1.6 mm, b=1.397 mm, h=0.127 mm, w1=0.1905 mm, w2=0.381 mm, $l$= 5.08 mm, $\epsilon_r$=2.2)

## IV. Conclusions

A unified theory has been presented for characterization of rectangular waveguide and microstrip discontinuities. To demonstrate the efficiency and versatility, many examples including waveguide open-end, right-angle bend and T-junction discontinuities and microstrip open-end and double-step discontinuities are examined. Most of the results are verified by the available published data and the simulations using currently popular software. In principle the proposed method can be used to analyze any three-dimensional metallic structures of irregular shape that are embedded in a multi-layered medium.

## References


[1] N. Marcuvitz, Waveguide Handbook, vol. 10 of MIT Rad, Lab. Series, McGraw-Hill, USA, 1966.

[2] T. Itoh, Numerical Techniques for Microwave and Millimeter-Wave Passive Structures, Wiely, USA, 1989.

[3] D.M. Pozar, Microwave Engineering, Addison-Wesley Publishing Company, USA, 1990.

[4] A. Wexler, "Solution of waveguide discontinuities by modal analysis," *IEEE Trans. Microwave Theory Tech.*, vol. MTT-15, pp. 508-517, 1967.

[5] H.Patzelt and F. Arndt, "Double-plane steps in rectangular waveguides and their applications for transformers, irises, and filters," *IEEE Trans. Microwave Theory Tech.*, vol. 30, pp. 771-776, May 1982.

[6] R.W. Jackson, "Full-wave finite element analysis of irregular microstrip discontinuities," *IEEE Trans. Microwave Theory Tech.*, vol. 37, pp. 81-89, Jan. 1989.

[7] S.C. Wu, H.Y. Yang, N.G. Alexopoulos, and I. Wolff, "A rigorous dispersive characterization of microstrip cross and T junctions," *IEEE Trans. Microwave Theory Tech.*, vol. 38, pp. 1837-1844, Dec. 1990.

[8] T.S. Horng, W.E. McKinzie, and N.G. Alexopoulos, "Full-wave spectral-domain analysis of compensation of microstrip discontinuities using triangular subdomain functions," *IEEE Trans. Microwave Theory Tech.*, vol. 40, pp. 2137-2147, Dec. 1992.

[9] J.R. Mosig, "Arbitrarily shaped microstrip structures and their analysis with a mixed potential integral equation," *IEEE Trans. Microwave Theory Tech.*, vol. MTT-36, pp. 314-323, Feb. 1988.

[10] K.A. Michalski and D. Zheng, "Analysis of microstrip resonators of arbitrary shape," *IEEE Trans. Microwave Theory Tech.*, vol. MTT-40, pp. 112-119, Jan. 1992.

[11] T. Becks and I. Wolff, "Analysis of 3-D metallization structures by a full-wave spectral-domain technique", *IEEE Trans. Microwave Theory Tech.*, vol. 40, pp. 2219-2227, Dec. 1992.

[12] T.S. Horng, "A rigorous study of microstrip crossovers and thier possible improvements," *IEEE Trans. Microwave Theory Tech.*, vol. 42, pp. 1802-1806, Sept. 1984.

[13] M.J. Tsai, C. Chen, N.G. Alexopoulos, and T.S. Horng, "Multiple arbitrary shape via-hole and air-bridge transitions in multilayered structures," *IEEE Trans. Microwave Theory Tech.*, vol. 44, pp. 2504-2511, Dec. 1996.

[14] M.J. Tsai, Via Hole Modeling for Multilayered Microstrip Circuits, Master's Thesis, University of California, Los Angeles, USA, 1993.

[15] T.S. Horng, "A Generalized method for evaluating the metallization thickness effects on microstrip structures," *IEEE MTT-S International Microwave Symposium Digest*, vol. 2, pp. 1009-1012, 1994.

[16] Q. Xu, K.J. Webb, and R. Mittra, "Study of modal solution procedures for microstrip step discontinuities," *IEEE Trans. Microwave Theory Tech.*, vol. 37, pp. 381-387, Feb. 1989.